Determining Skin Zone Properties from Injectivity Tests in Single and Multilayer Reservoirs

Renan Vieira Bela[a,*], Sinesio Pesco[a], Abelardo Barreto Jr.[a]

[a]*PUC-Rio, Departamento de Matemática*

Abstract

This work proposes an interpretation technique for injectivity tests that provides a new estimation for skin zone permeability and radius in single-layer reservoirs. A means to compute the reservoir skin factor in multilayer commingled reservoirs is also presented. Under the assumption that layer flow-rates are decoupled, the suggested method was extended to compute individual layer permeabilities and skin factors. Results indicate that this hypothesis is valid in reservoirs where layer skin factors are similar.

Keywords: Injectivity Test, Parameter Estimation, Skin Properties, Commingled Systems

1. Introduction

Perforation and completion of the wellbore might either impair or stimulate flow around the wellbore, forming a region with modified permeability. Hence, an additional pressure change occurs. Properties inside this damaged region are grouped in a parameter called mechanical skin factor, which is defined as [1]:

$$S = \left(\frac{k}{k_{skin}} - 1\right) ln\left(\frac{r_{skin}}{r_w}\right), \qquad (1)$$

where k stands for the reservoir permeability, r_w represents the wellbore radius, k_{skin} and r_{skin} denote the damaged zone permeability and radius, respectively.

As equation (1) shows, an infinite number of radius-permeability combinations yields the same skin factor.

Even though conventional analysis techniques are able to determine the reservoir skin factor [2, 3, 4, 5], they cannot provide estimates for skin zone permeability and radius. Multilayer reservoirs present an additional setback, since skin zone properties may not be the same in all layers. Thus, additional information must be obtained from the pressure transient test, so that the damaged region properties can be determined.

During an injectivity test, the pressure derivative profile presents a characteristic signature, associated with the development of the flooded region [6, 7, 8]. Thereby, pressure derivative profile indicates the time when the waterfront overcomes the damaged zone in single-layer reservoirs. Skin radius, then, may be estimated using

*I am corresponding author

Email addresses:

renanvb1@aluno.puc-rio.br (Renan Vieira Bela), sinesio@puc-rio.br (Sinesio Pesco), abelardo.puc@gmail.com (Abelardo Barreto Jr.)

Buckley-Leverett theory [9].

In this context, the first contribution of this work is to develop a technique to determine the skin zone radius in single-layer reservoirs. Then, skin zone permeability may also be computed, provided that an estimation for the mechanical skin factor is available.

Furthermore, an attempt was made to extend the proposed method to evaluate individual layer permeability, skin factor and damaged zone properties in multilayer reservoirs. Computation of individual layer properties was developed by assuming that layer flow-rates are decoupled. The discussion over the validity of this hypothesis is perhaps the most relevant novelty in this work.

Section 2 presents a brief overview on the existing analytical model for water injection in a reservoir composed of any number of layers. Section 3 depicts the suggested technique to compute damaged zone properties in single-layer reservoirs, while the formulation for multilayer systems is described in sections 4 and 5. The proposed method was applied on a set of cases, whose results are displayed in section 6. Finally, the main conclusions of this work may be seen in section 7.

2. Mathematical Model

Pressure change during an injectivity test can be understood as the sum of two terms; one related to the single-phase oil displacement [8]. During the injection period, pressure change in reservoirs without formation damage is given by [7]:

$$\Delta P_{wf}(t) = \Delta P_o(t) + \frac{q_{inj}}{\sum_{j=1}^{n} A_j^{-1}(t)} \quad (2)$$

The $\Delta P_o(t)$ term is evaluated by the line source solution [5]. At late times, it can be estimated by the following logarithmic approximation [4]:

$$\Delta P_o(t) = \frac{\alpha_p q_{inj}}{2 k_{eq} h_T \hat{\lambda}_o} ln\left(\frac{4\alpha_t k_{eq} \hat{\lambda}_o}{e^{\gamma} \phi c_t r_w^2} t\right) \quad (3)$$

Equation (3) assumes that porosity and total compressibility are the same in all layers. If that is not the case, the ϕc_t product may be replaced by a thickness averaged porosity-compressibility product.

The $A_j(t)$ coefficient is a weighting variable that encompasses the mobility contrast between oil and water in a given layer j [7]:

$$A_j(t) = \frac{\alpha_p}{k_j \hat{\lambda}_o h_j} \int_{r_w}^{r_{Fj}(t)} \left(\frac{\hat{\lambda}_o}{\lambda_t} - 1\right) \frac{dr}{r} \quad (4)$$

Buckley-Leverett theory is applied to compute the waterfront radius r_{Fj} [9]:

$$r_{Fj}(t) = \sqrt{\frac{q_j f'_w t}{24\pi\phi h_j} + r_w^2} \quad (5)$$

In reservoirs with formation damage, an additional term must be added to account for the mechanical skin:

$$\Delta P_{wf}(t) = \Delta P_o(t) + \frac{q_{inj}}{\sum_{j=1}^{n} A_j^{-1}(t)} + \Delta P_{skin} \quad (6)$$

The ΔP_{skin} term depicts how the skin zone affects the single-phase oil flow. It is defined as:

$$\Delta P_{skin} = \frac{\alpha_p q_{inj}}{k_{eq} h_T \hat{\lambda}_o} S \quad (7)$$

In multilayer reservoirs, the skin factor is given by a weighted average of individual layer skin factors [2], which are computed according to equation (1):

$$S = \frac{\sum_{j=1}^{n} q_j S_j}{q_{inj}} \tag{8}$$

Although layer mechanical skins are constant, layer flow-rates may vary in time [2, 7]. Thus, according to equation (8), the reservoir skin factor can also change in time. That is, it accounts for the flow-rate transient effects.

The damaged zone also influences the two-phase flow that occurs within the flooded region. Thereby, the expression for the $A_j(t)$ coefficient changes, and depends on whether or not the flooded region has overcome the skin radius. While the waterfront is within the damaged zone:

$$A_j(t) = \frac{\alpha_p}{k_{j_{skin}} \hat{\lambda}_o h_j} \int_{r_w}^{r_{Fj}(t)} \left(\frac{\hat{\lambda}_o}{\lambda_t} - 1 \right) \frac{dr}{r} \tag{9}$$

Otherwise:

$$A_j(t) = \frac{\alpha_p}{k_j h_j \hat{\lambda}_o} \left[\int_{r_w}^{r_{Fj}(t)} \left(\frac{\hat{\lambda}_o}{\lambda_t} - 1 \right) \frac{dr}{r} + \left(\frac{k_j}{k_{j_{skin}}} - 1 \right) \int_{r_w}^{r_{j_{skin}}} \left(\frac{\hat{\lambda}_o}{\lambda_t} - 1 \right) \frac{dr}{r} \right] \tag{10}$$

3. Determining Skin Zone Properties in Single-Layer Reservoirs

In single-phase well testings, the mechanical skin factor is determined from the difference between the observed pressure at a given time and the pressure change that would be expected if there were no formation damage [2]. Pressure change for the zero skin case is estimated by equation (3).

In injectivity tests, besides the mechanical skin due to the formation damage, there is also an apparent skin, that reflects the mobility contrast between oil and water. Hence, the procedure described above yields a total skin factor, which encompasses both mechanical and apparent skins [6]. Thus:

$$S_t(t) = \frac{kh\hat{\lambda}_o}{\alpha_p q_{inj}} \left(\Delta P_{wf}(t) - \Delta P_o(t) \right) \tag{11}$$

The relation between total, apparent and mechanical skin is given by [6]:

$$S_t(t) = S_{ap}(t) + \frac{S}{\hat{M}} \tag{12}$$

In equation (12), $\hat{M}$ stands for the endpoint mobility ratio. It measures the relative easiness of water and oil to flow throughout the reservoir and is defined as the ratio between water and oil endpoint mobilities:

$$\hat{M} = \frac{\hat{\lambda}_w}{\hat{\lambda}_o} \tag{13}$$

The mechanical skin depends only on the damaged zone properties, which do not vary in time. Thus, the mechanical skin remains constant in time. The apparent skin, in its turn, depends on the waterfront radius, which increases as injection goes on:

$$S_{ap}(t) = \int_{r_w}^{r_F(t)} \left(\frac{\hat{\lambda}_o}{\lambda_t} - 1 \right) \frac{dr}{r} \tag{14}$$

Therefore, the apparent skin changes in time. Hence, so does the total skin factor, as displayed in equation (12).

Equations (11) to (14) portray how the mechanical skin is determined. Nevertheless, equation (1) shows that, for a given skin factor, there are infinite possible combinations of skin zone radius and permeability. Thereby, estimates for skin zone properties have been unachievable so far.

Pressure derivative behavior, however, can help to accomplish this task. As depicted in section 2, the formulation to compute the $A_j(t)$ coefficient changes according to the waterfront radius. As the flooded region reaches the skin zone radius, equation (9) is no longer valid and equation (10) must be used to compute the pressure change.

This causes a characteristic signature in the derivative profile. A sharp shift in pressure derivative is identified when the waterfront overcomes the skin radius. Figure 1 illustrates the time when a blunt drop in pressure derivative is observed, in a reservoir with endpoint mobility ratio lower than 1. Reservoir properties are the same as case A, depicted in table 1.

Thereby, the time required for the waterfront to reach the damaged zone radius (from now on denoted as t_s) may be obtained from the pressure derivative profile. Once t_s has been identified, skin zone radius may be estimated using Buckley -Leverett's theory [9]:

$$r_{skin} = \sqrt{\frac{q_{inj} f'_w t_s}{24\pi\phi h} + r_w^2} \qquad (15)$$

In cases where flow is favorable to water, there might occur a pressure drop after the waterfront overcomes the damaged region. Pressure derivative, then, decreases and may even assume negative values. Besides, the shift in pressure derivative behavior may not be so easily identifiable because the water saturation profile is smoother. Figure 2 shows the pressure and pressure derivative behavior for case B, from table 1, which is an example with mobility ratio favorable to water. In these cases, the time when pressure derivative attains its minimum value should be assigned as t_s.

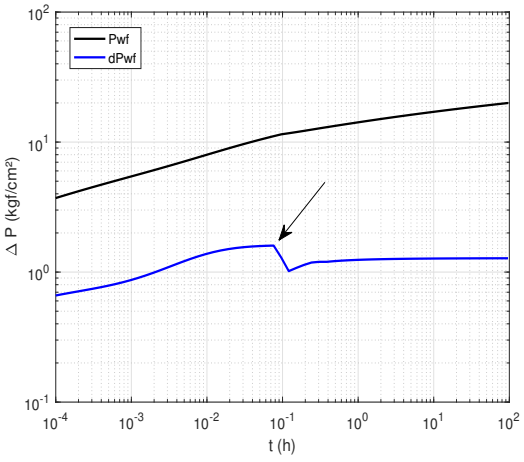

Figure 1: Pressure and Derivative Data for Case A

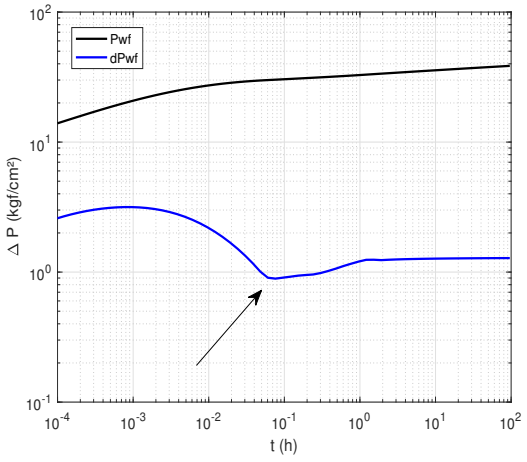

Figure 2: Pressure and Derivative Data for Case B

Lastly, skin zone permeability might be determined through equation (1), applying the previously computed values for the mechanical damage and skin radius. Reservoir permeability, which is also required by equation (1), is estimated from the constant pressure derivative level [4, 8]:

$$k = \frac{1.151 \alpha_p q_{inj}}{h \hat{\lambda}_f m_f}, \tag{16}$$

where f denotes either water or oil and m_f is the constant pressure derivative level associated to phase f.

4. Computing the Reservoir Skin Factor in Multilayer Reservoirs

The procedure depicted in section 3 may be applied to evaluate the reservoir skin factor in multilayer reservoirs, with some suitable adjustments.

Assuming that oil properties are the same in all layers, total skin factor is computed by using the reservoir equivalent permeability and total thickness in equation (11):

$$S_t(t) = \frac{k_{eq} h_T \hat{\lambda}_o}{\alpha_p q_{inj}} \left(\Delta P_{wf}(t) - \Delta P_o(t) \right) \tag{17}$$

The computation of the apparent skin, depicted in equation (14), requires a waterfront radius. This radius may be obtained using the total injection flow-rate and the reservoir total thickness in equation (5), provided that all layers present the same relative permeability curves:

$$r_F(t) = \sqrt{\frac{q_{inj} f'_w t}{24 \pi \phi h_T} + r_w^2} \tag{18}$$

The mechanical skin, then, may be evaluated through equation (12).

It is important to notice, though, that the waterfront may propagate differently in each layer, as shown in figure 3. Therefore, the waterfront radius from equation (18) does not necessarily correspond to the waterfront in any given layer.

Instead, it is a theoretical radius, which is required to set the integral limit in equation (14). Since relative permeability curves are assumed to be the same in all layers, then this theoretical waterfront radius allows the determination of the reservoir apparent skin, as described in equation (14), without further concerns.

5. Estimating Individual Layer Properties

An attempt is also made to estimate individual layer properties. Here, a crucial hypothesis is that flow is decoupled with respect to each layer, and flow-rates stabilize at a level proportional to layer flow capacities after a short transient period. For single-phase flow in commingled systems, it is known that this condition holds [3, 10].

Under the assumption that injection in each layer is independent of the

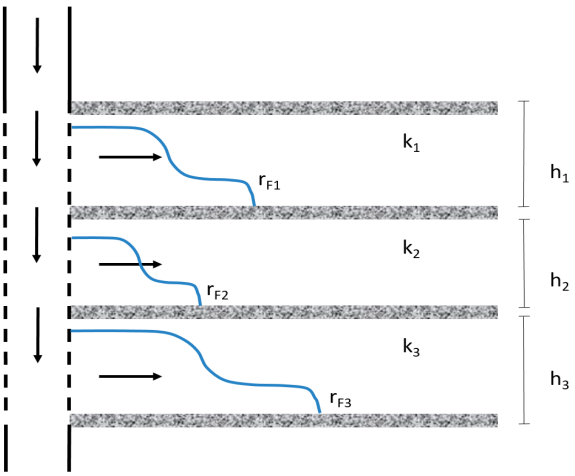

Figure 3: Waterfront Propagation in Each Layer

others, reservoir properties in equation (17) should be replaced by the respective layer properties to estimate total skin in a given layer j:

$$S_{t_j}(t) = \frac{k_j h_j \hat{\lambda}_o}{\alpha_p q_j} \left(\Delta P_{wf}(t) - \Delta P_{o_j}(t) \right) \quad (19)$$

Since flow is assumed to be decoupled in each layer, the ΔP_{o_j} term in equation (19) should be evaluated using the properties from layer j:

$$\Delta P_{o_j}(t) = \frac{\alpha_p q_j}{2 k_j h_j \hat{\lambda}_o} ln \left(\frac{4 \alpha_t k_j \hat{\lambda}_o}{e^{\gamma} \phi c_t r_w^2} t \right) \quad (20)$$

The decoupled flow-rates hypothesis enables the estimation of layer permeability as well. The suggested computation derives directly from the determination of the reservoir equivalent permeability:

$$k_j = \frac{1.151 \alpha_p q_j}{h_j \hat{\lambda}_f m_f} \quad (21)$$

Layer apparent skin is computed through equation (14), using the waterfront radius foreseen by equation (5). After total and apparent skin in a given layer have been computed, the mechanical skin will be evaluated, once again, by equation (12). One should notice that equations (12) and (14) are not affected by the decoupled flow-rates hypothesis.

To estimate layer skin zone radius, the value of t_s should be defined in an analogous way to the single-layer case. Then, skin zone radius is determined by applying the identified value of t_s in equation (5).

In multilayer reservoirs, it is important to notice that there might occur more than one sharp shift in the pressure derivative profile. This signs that layer skin zone properties are remarkably different and, therefore, it takes more time for the damaged region in one layer to be overcome by the waterfront than in another layer. In these cases, more than one value of t_s might be identified. In a field example, where layer properties are unknowns to be determined, it is impracticable to identify which blunt shift is related to which layer.

5.1. Assessing the Validity of the Decoupled Flow-Rates Hypothesis

Equations (19) and (21) highlight that the estimates for layer skin factor and permeability, which are constant, depend on layer flow-rate, which may vary in time.

In fact, the reservoir mechanical skin defined by equation (8) indicates that layer flow-rates are indeed coupled. Moreover, the formulation for the injection period in multilayer reservoirs under two-phase flow, developed by Barreto *et al.* [7], also suggests that flow in each layer is indeed dependent of the other layers:

$$q_j(t) = \frac{\Delta P_{wf}(t) - \Delta P_o(t) - \Delta P_{skin}}{A_j(t)} \quad (22)$$

Whenever the decoupled flow-rate hypothesis is valid, equation (22) must yield the expected steady-state flow-rate according to layer flow capacities.

Thus, replacing equation (6) in equation (22):

$$q_j(t) = \frac{1}{A_j(t)} \frac{q_{inj}}{\sum_{i=1}^{n} A_j^{-1}(t)} \quad (23)$$

The goal is to study the conditions required for flow-rates in all layers to stabilize at a level proportional to its flow capacity. For this reason, it is more relevant to understand flow-rate behavior after the

waterfront has overcome the damaged zone in all layers. Thereby, applying equation (10) in expression (23):

$$q_j(t) = \frac{1}{\frac{\alpha_p}{k_j \hat{\lambda}_o h_j} b_j} \frac{q_{inj}}{\sum_{i=1}^{n} \left[\frac{\alpha_p}{k_i \hat{\lambda}_o h_i} b_i\right]^{-1}} \tag{24}$$

In equation (23), b_j is a coefficient that encompasses both integral terms in the definition of $A_j(t)$:

$$b_j = S_{apj} + \left(\frac{k_j}{k_{j_{skin}}} - 1\right) \int_{r_w}^{r_{j_{skin}}} \left(\frac{\hat{\lambda}_o}{\lambda_t} - 1\right) \frac{dr}{r} \tag{25}$$

In section 2, oil properties and relative permeability curves have been assumed to be the same in all layers. Applying this assumption in equation (24):

$$q_j(t) = \frac{1}{\frac{b_j}{k_j h_j}} \frac{q_{inj}}{\sum_{i=1}^{n} \frac{k_i h_i}{b_i}} \tag{26}$$

Hence, if the b_j term is the same in all layers, equation (26) may be rewritten as:

$$q_j(t) = q_{inj} \frac{k_j h_j}{\sum_{i=1}^{n} k_i h_i} = q_{ss_j} \tag{27}$$

Equation (27) shows that, under the assumptions made, flow-rate in a given layer remains constant after the waterfront in every layer has overcome the skin radii. Layer flow-rate, then, stabilizes at a level proportional to layer flow capacity, as would be expected in a single-phase flow [3, 10]. This flow-rate is denoted as q_{ss_j}.

Therefore, the decoupled flow-rate hypothesis is applicable whenever b_j is approximately the same in all layers. In other words, the method portrayed in this section yields good estimates for individual layer properties whenever layer properties are not remarkably different, specially within the damaged region.

If that is not the case, then layer flow-rate may stabilize at a level completely different than q_{ss_j}. The reason for that dwells on the expression to compute b_j. Using the definition for layer mechanical skin (eq. (1)), equation (25) may be rewritten as:

$$b_j = S_{ap_j} + \frac{S_j}{\ln\left(\frac{r_{j_{skin}}}{r_w}\right)} \int_{r_w}^{r_{j_{skin}}} \left(\frac{\hat{\lambda}_o}{\lambda_t} - 1\right) \frac{dr}{r} \tag{28}$$

Applying equation (8) in equation (28):

$$b_j = S_{ap_j} + \frac{q_{inj} S}{q_j \ln\left(\frac{r_{j_{skin}}}{r_w}\right)} \int_{r_w}^{r_{j_{skin}}} \left(\frac{\hat{\lambda}_o}{\lambda_t} - 1\right) \frac{dr}{r} \tag{29}$$

Thus, equations (26) and (29) evidence that layer flow-rates are in fact coupled when layer properties are different enough so that the b_j term may not be assumed to be approximately equal in all layers.

A possible alternative to overcome this setback could be achieved by using the rate normalized pressure change to estimate individual layer properties. This technique was presented by Ehlig-Economides and Joseph [3] for multilayer commingled reservoirs under conventional well testing.

However, to apply their formulation, there must be a flow-rate change during the test, so that two different non-zero flow-rates occur. Parameters, then, are computed based on the rate normalized pressure change. In injectivity tests, a

Case	q_{inj} (m^3/d)	k (mD)	h (m)	k_{skin} (mD)	r_{skin} (m)	S	ϕ	μ_o (cP)
A	500	400	30	250	0.30	0.80	0.32	1.0
B	500	400	30	250	0.30	0.80	0.32	5.1
C	400	600	25	100	0.40	7.74	0.20	4.8
D	400	600	25	100	0.40	7.74	0.20	1.2
E	200	750	20	400	0.25	1.05	0.12	5.5
F	300	500	25	250	0.30	1.33	0.18	0.8
G	500	1000	30	1200	0.50	-0.29	0.32	5.1
H	500	1000	30	1200	0.50	-0.29	0.32	1.0

Table 1: Single-Layer Cases Properties

variable flow-rate would imply in great difficulties to compute waterfront radii. Thereby, their method is not easily adapted to injectivity tests.

6. Results and Discussion

The techniques described in sections 3 to 5 were applied on a set of cases in order to assess their accuracy. For all cases, water viscosity was set as 0.52 cP, which is the typical water viscosity at the reservoir temperature. It was considered an injection time of 96 h (or 4 days), followed by a falloff time of 96h. Falloff pressure data was used to determine reservoir and layer permeabilities. Wellbore radius was 0.108m. Relative permeability curves, rock and fluid compressibilities were extracted from Bela *et al.* [8].

6.1. Single-Layer Cases

Table 1 presents the reservoir features for the single-layer tested cases, while table 2 show the results obtained applying the proposed method in these cases. In both tables, the skin zone radii denotes the damaged zone extension beyond the wellbore.

Cases A to F consists of cases where flow around the wellbore is impaired; that is, skin factor is positive. Cases G and H, in their turn, represent reservoirs where flow around the wellbore is stimulated. This might happen, for example, in some carbonate reservoirs.

The suggested technique was able to provide estimates for skin zone properties in all cases, except case G. In this case, the mobility ratio is favorable to water. This means that the waterfront shape is smoother and, hence, the pressure derivative shift is softened. Besides, positive mechanical skins also impair the detection of t_s. For those reasons, no noticeable pressure derivative shift was observed in case G. Thus, skin zone radius was not computed. Pressure and pressure derivative profile for this case are displayed in figure 4. It is interesting to observe, though, that the mobility ratio in case H was favorable enough to oil so that t_s could be identified. In all other cases the value of t_s could be identified from the pressure derivative profile as depicted in section 3.

Case B presented the highest error for the skin radius estimate. There are two main causes for that. The first is the mobility ratio. As explained regarding case G, mobility ratios favorable to water imply in a smoother waterfront profile. This means that the shift in pressure derivative is

Case	S	Error (%)	k (mD)	Error (%)	t_s (h)	r_{skin} (m)	Error (%)	k_{skin} (mD)	Error (%)
A	0.78	-2.8	399	-0.3	0.10	0.30	0.4	252	0.9
B	0.77	-3.0	402	0.5	0.08	0.34	13.8	261	4.3
C	7.65	-1.2	602	0.3	0.06	0.37	-6.8	98	-1.7
D	7.54	-2.7	599	-0.1	0.08	0.38	-3.9	100	0.4
E	1.02	-2.9	752	0.2	0.03	0.27	7.3	414	3.5
F	1.20	-9.6	499	-0.1	0.06	0.29	-2.8	26	4.1
G	-0.30	4.9	1002	0.2	–	–	–	–	–
H	-0.29	2.4	999	-0.1	0.24	0.53	5.4	1199	-0.1

Table 2: Estimated Skin Zone Properties of the Single-Layer Cases

not so easily identified. Additionally, higher mobility ratios imply that the waterfront will overcome the damaged region faster. Thereby, the detection of t_s in cases with mobility ratio favorable to water is more sensitive to the time discretization.

Furthermore, the shorter the skin zone radius, the faster the waterfront will overcome the damaged region. This means that shorter skin radii increase the method sensitivity to the time discretization as well. These two reasons also explain why skin radii presented higher errors in cases C and E.

On the other hand, cases A, D, F and H presented either a mobility ratio favorable to oil, or longer skin zone radius, or both. As a result, errors associated to skin zone estimates were lower in these cases.

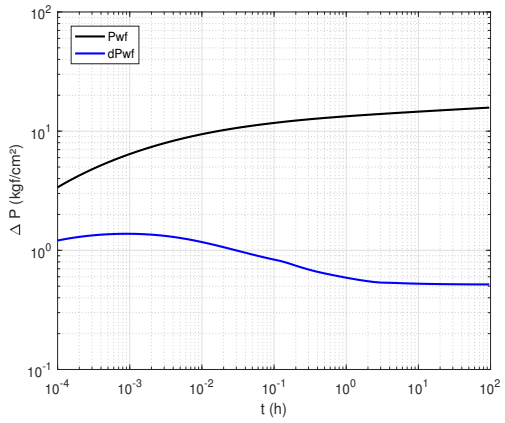

Figure 4: Pressure and Derivative Data for Case G

Regardless the issues related to the skin radii computation, permeability inside the damaged region was accurately estimated in all cases. The reason for this fact dwells on how skin permeability is evaluated. As equation (1) shows, the estimation of skin zone permeability depends not only on the skin radius, but also on the mechanical skin factor and reservoir permeability. Thus, even in cases where skin radius error were more relevant, the estimates for k_{skin} were computed with good accuracy due to the reservoir skin factor and permeability.

6.2. Multilayer Cases

Reservoir properties of the multilayer cases are displayed in table 3. Table 3 also shows the expected steady-state flow-rate in each layer (q_{ss_j}), evaluated according to layer flow capacities, as proposed by Spath *et al.* [10]. Estimates for layer properties are reported in table 4, while the computed reservoir skin factors may be seen in table 5. Permeability inside the damaged region was estimated using the computed values for k_j and $r_{j_{skin}}$ in

Case	q_{inj} (m^3/d)	ϕ	μ_o (cP)	Layer	k_j (mD)	h_j (m)	$k_{j_{skin}}$ (mD)	$r_{j_{skin}}$ (m)	S_j	q_{ss_j} (m^3/d)
I	200	0.12	1.0	1	600	10	240	0.25	1.80	100
				2	600	10	–	–	–	100
J	500	0.32	5.1	1	1000	15	500	0.50	1.73	250
				2	1000	15	100	0.50	15.6	250
K	100	0.25	2.3	1	600	15	150	0.20	3.14	53
				2	800	10	200	0.20	3.14	47
L	400	0.30	0.8	1	500	12	600	0.30	-0.22	261
				2	400	8	480	0.40	-0.26	139
M	500	0.20	4.8	1	1500	10	500	0.40	3.10	259
				2	500	12	–	–	–	103
				3	1000	8	–	–	–	138
N	400	0.15	1.5	1	1000	10	250	0.40	4.65	159
				2	1200	8	400	0.50	3.46	152
				3	800	7	300	0.20	1.75	89

Table 3: Multilayer Cases Properties

equation (1). Once again, skin zone radii denote the damaged zone extension beyond the wellbore radius. Actual reservoir skin factors were determined through equation (8), applying the last measured flow-rate in each layer (which may be observed in table 4).

In the multilayer examples, each case presented some particular features that deserve a more detailed comment. For this reason, a brief analysis regarding each case will be made:

Case I: in this example, both layers present the same properties, except for the formation damage, which affects only layer 1. For this reason, layer flow-rates stabilize at a level that do not correspond to their respective steady-state values. Difference between measured and expected steady-state flow-rates is directly reflected in the errors presented by estimated layer permeabilities: the difference between q_j and q_{ss_j} is approximately equal to the layer permeability error for both layers. This result indicates that the decoupled flow-rates hypothesis is more sensitive to skin zone properties than to layer permeabilities. It is interesting to notice, though, that the proposed method was able to compute the skin factor for layer 1 with good accuracy and yielded a low skin factor for layer 2, which actually presents no skin. The reservoir mechanical skin was also estimated with low error.

As depicted in section 4, the value identified for t_s was applied to determine the skin zone radius in both layers. Since layer 2 presents no formation damage, it was expected that the estimated skin zone permeability in this layer would be very close to the actual layer permeability, implying that $S_2 \simeq 0$. However, estimated skin zone properties for both layers showed a significant error. In layer 1, the estimation of skin zone radius is subject to the same issues as the single-layer cases. Once again, time discretization plays an important role. Accuracy of skin zone permeability, in

Case	Layer	q_j (m^3/d)	k_j (mD)	Error (%)	S_j	Error (%)	t_s (h)	$r_{j_{skin}}$ (m)	Error (%)	$k_{j_{skin}}$ (mD)	Error (%)
I	1	88	530	-11.7	1.95	8.6	0.06	0.28	12.1	210	-12.5
	2	112	669	11.5	-0.16	–		0.32	–	758	–
J	1	381	1527	52.7	-2.12	-222.8	0.19	0.75	50.5	-68668	-13833
	2	119	477	-52.3	27.53	77,0		0.38	-23.8	25	-75.2
K	1	53	606	1.0	3.01	-4.3	0.19	0.23	13.6	166	10.5
	2	47	791	-1.1	3.16	0.4	0.12	0.20	-0.2	197	-1.5
L	1	258	494	-1.2	-0.24	7.8	0.08	0.35	17.5	591	-1.5
	2	142	406	1.5	-0.32	23.4		0.31	-22.0	530	10.5
M	1	190	1104	-26.4	6.98	125.5	0.08	0.48	18.8	215	-57.0
	2	138	669	33.7	-2.52	–		0.35	–	-899	–
	3	172	1246	24.6	-2.01	–		0.51	–	-8309	–
N	1	147	925	-7.5	4.36	-6.1	0.02	0.22	-44.8	188	-24.7
	2	149	1171	-2.4	3.54	2.3		0.26	-48.4	30	-24.9
	3	104	938	17.3	1.53	-12.4		0.22	11.5	396	32.1

Table 4: Estimated Layer Properties of the Multilayer Cases

Case	S_{real}	$S_{est.}$	Error(%)
I	0.79	0.77	-2.6
J	5.02	4.79	-4.6
K	3.14	3.08	-2.0
L	-0.23	-0.26	12.9
M	1.18	1.23	4.7
N	3.45	3.32	-3.8

Table 5: Estimated Reservoir Mechanical Skin for the Multilayer Cases

its turn, depends not only on the skin zone radius, but also on layer permeability and skin factor. As mentioned, layer permeability could not be evaluated with a good accuracy, and the error propagated to the skin zone permeability. This explains the error observed in layer 2 as well.

Case J: This example clearly highlights the limitations of the proposed technique for layer properties determination. Here both layers present the same properties, expect for the skin zone permeability (and, hence, the mechanical skin). As a result, layer flow-rates remained during all test far from their expected flow capacity level. Thus, no layer property could be estimated with an acceptable error. This reinforces that, whenever layer skin factors are remarkably different, layer flow-rates are coupled and the suggested method is no longer applicable. Yet, the reservoir mechanical skin was estimated with good accuracy, showing once more that the method described in section 4 is independent of layer flow-rate history

Case K: This example presented the best results from all multilayer tested cases. This better accuracy derives from the flow-rate history. The values for q_{ss_j} and q_j in tables 3 and 4 evidence that layer flow-rates converged to the level associated with layer flow capacities. Thus, layer skin factors and permeabilities were evaluated with good accuracy. The reservoir skin factor was also estimated with little error. These results also suggest that layer skin zone properties are more relevant to the

decoupled flow-rates hypothesis than layer permeabilities, which is consistent with cases I and J.

Pressure derivative in this example, portrayed in figure 5, presented two blunt shifts. Since the reservoir presents 2 layers, both pressure derivative drops were used to assign 2 values of t_s. The first time was applied to compute the skin zone radius for the second layer, because this layer presents higher skin zone permeability and, hence, it should take a shorter time for the waterfront to overcome the damaged zone in this layer. Estimated values for $r_{j_{skin}}$ indicate that this assumption was correct and the first derivative drop is indeed related to the second layer. However, in a practical case, it is impossible to state with certainty that a given derivative shift is associated to a given layer, due to the fact that an infinite number of skin zone radius-permeability combinations yield the same skin factor, as depicted by equation (1).

Case L: This stimulated example yielded good results for layer permeabilities. Again, this is explained by layer flow-rate history, which stabilized at the level foreseen by layer flow capacities. Here, only one sharp shift was observed in the pressure derivative profile. Thereby, skin zone radii for both layers were estimated using the same value for t_s. Results suggest that the waterfront overcome the damaged zones approximately at the same time and, thus, the derivative shifts associated to each layer overlap one another. Therefore, estimates for skin zone properties presented relevant errors.

Case M: This example also consists of a reservoir where only one layer presents formation damage. But here, layers present distinct permeabilities and thickness. Flow-rate history, displayed in figure 6, evidences that all layer flow-rates stabilize at a level which is completely different than what would be expected according to the flow capacity in each layer. This flow-rate profile is explained by the difference between layer skin factors.

As a result, layer properties in this case were estimated with significant error. Computed mechanical skin for layers 2 and 3 - which do not present skin effect - were quite relevant, unlike case I, where the estimated skin factor for the layer without formation damage was small. These results strengthens that the proposed method relies

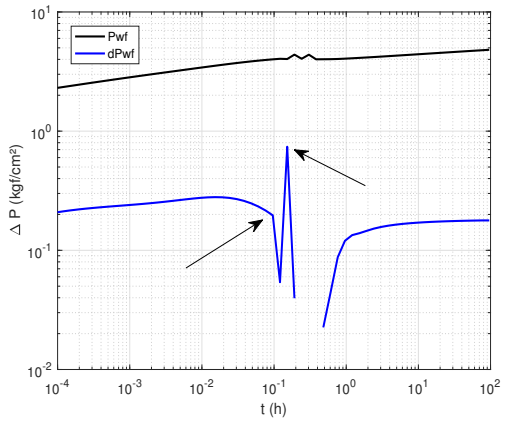

Figure 5: Pressure and Derivative Data for Case K

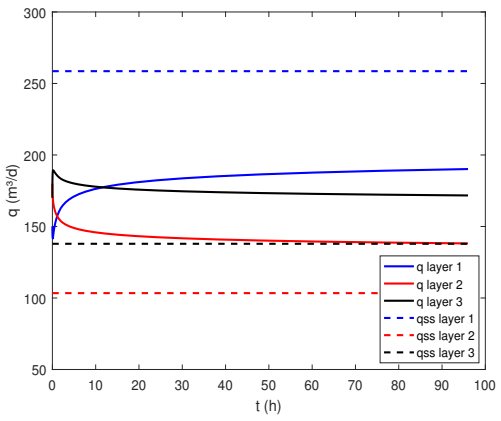

Figure 6: Layer Flow-Rate History for Case M

on the fact that layer flow-rate must have reached the level foreseen by its flow capacity.

Computation of the reservoir skin factor, in its turn, was close to the actual value. This indicates that, although the proposed technique for layer properties estimation is sensitive to flow-rate transient effects (depicted in section 5), the same does not hold when it comes to determining the reservoir skin factor (reported in section 4).

Case N: Analysis of this case is much similar to case M. The reservoir mechanical skin was computed with good accuracy, despite the fact that, once again, layer flow-rates stabilized at a level that is not related to layer flow capacity. On the other hand, this case exhibited an interesting feature regarding the determination of t_s.

Figure 7 shows the pressure and pressure derivative profile for case N. Two distinct sharp drops in pressure derivative profile may be clearly identified in figure 7, as in case K. However, since the reservoir consists of three layers, the third shift must be partially or totally overlapped with one of the two observed drops. As it is impossible to state *a priori* which shift is related to each layer, all skin zone radii were computed using the time of the first derivative drop as t_s. Results suggest that this value of t_s is associated to the third layer. Nevertheless, it is important to remind that in a real field case one can not assure which layer matches the pressure derivative shift.

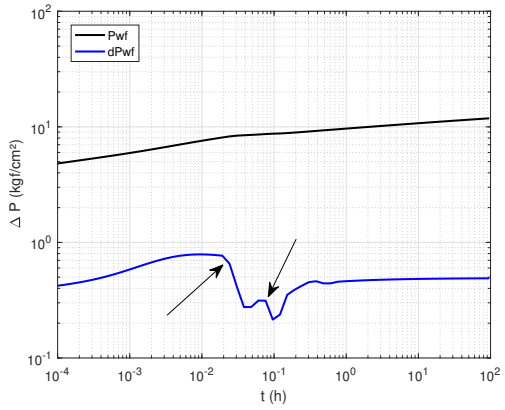

Figure 7: Pressure and Derivative Data for Case N

7. Conclusions

Based on the analytical formulation for the injection period, an interpretation method was developed to estimate the skin zone radius in single-layer reservoirs. Damaged zone permeability may also be computed, provided that the reservoir mechanical skin has been determined.

The proposed technique was applied on a set of cases, and presented good results. The suggested method was more accurate for greater skin radii and lower endpoint mobility ratios.

For multilayer commingled reservoirs, a means for determining the reservoir mechanical skin was achieved. Assuming that layer flow-rates are decoupled, an attempt was also made to estimate individual permeabilities and layer skin factors. Results indicate that, whenever layer skin factors are similar, the decoupled flow-rates hypothesis is valid and the suggested method yields good estimates.

In multilayer systems, the blunt pressure derivative shifts associated to each layer may be overlapped. Besides, in a practical case, it is not possible to state with certainty which shift is associated to which layer. Thus, estimated skin zone properties presented significant errors.

Nomenclature

c_t = Total compressibility
$f_w^{'}$ = Fractionary flow derivative

h_j = Thickness of layer j
h_T = Reservoir total thickness
k_{eq} = Reservoir equivalent permeability
k_j = Permeability in layer j
$k_{j_{skin}}$ = Skin zone permeability in layer j
$\hat{M}$ = Endpoint mobility ratio
P_{wf} = Wellbottom hole pressure
q_{inj} = Injection flow-rate
q_j = Flow-rate in layer j
r_{Fj} = Waterfront radius in layer j
$r_{j_{skin}}$ = Skin zone radius in layer j
r_w = Wellbore radius
S = Mechanical skin factor
S_{ap} = Apparent skin
S_j = Skin factor of layer j
S_t = Total skin
S_{t_j} = Total skin in layer j
t = Time
α_p = Pressure unit conversion constant
α_t = Time unit conversion constant
γ = Euler constant
$\hat{\lambda}_o$ = Endpoint oil mobility
$\hat{\lambda}_w$ = Endpoint water mobility
λ_t = Total mobility
ϕ = Porosity

Acknowledgements

Authors are grateful to Petrobras for partially sponsoring this research. This study was financed in part by the Coordenação de Aperfeiçoamento de Pessoal de Nível Superior - Brasil (CAPES) - Finance Code 001

References

[1] HAWKINS, M. F, A Note on the Skin Effect, Journal of Petroleum Technology December (1956) 65–66.

[2] GAO C., Determination of Parameters for Individual Layers in Multilayer Reservoirs by Transient Well Tests, SPE Formation Evaluation March (1987) 43–65.

[3] EHLIG-ECONOMIDES, C. A.; JOSEPH, J., A New Test for Determination of Individual Layer Properties in a Multilayered Reservoir, SPE Evaluation Formation September (1987) 261–283.

[4] BANERJEE, R.; THOMPSON, L. G.; REYNOLDS, A. C., Injection/Falloff Testing in Heterogeneous Reservoirs, SPE Reservoir Evaluation & Engineering December (1998) 519–527.

[5] PERES, A. M. M.; BOUGHARA, A. A.; CHEN, S.; MACHADO, A. A. V.; REYNOLDS. A. C., Approximate Analytical Solutions for the Pressure Response at a Water Injection Well, Paper presented at the Annual Technical Conference and Exhibition September (2004) 1–17.

[6] PERES, A. M. M.; BOUGHARA, A. A.; REYNOLDS, A. C., Rate Superposition for Generating Pressure Falloff Solutions, SPE Journal September (2004) 364–374.

[7] BARRETO JR, A.; PERES, A.; PIRES, A., Water Injectivity Tests on Multilayered Oil Reservoirs, Paper presented at the Brasil Offshore Conference and Exhibition 524 (2011) 1–11.

[8] BELA, R. V., PESCO, S., BARRETO JR., A., Modeling Falloff Tests in Multilayer Reservoirs, Journal of Petroleum Science and Engineering 174 (2019) 161–168.

[9] BUCKLEY, S. E.; LEVERETT, M. C., Mechanism of Fluid Displacement in Sands, Petroleum Technology May (1941) 107–116.

[10] SPATH, J. B., OZKAN, E., RAGHAVAN, R., An Efficient Algorithm for Computation of Well Responses in Commingled Reservoirs, SPE Formation Evaluation June (1994) 115–121.